



# Recipient-Biased Competition for an Intracellularly Generated Cross-Fed Nutrient Is Required for Coexistence of Microbial Mutualists

Alexandra L. McCully, Breah LaSarre, James B. McKinlay

Department of Biology, Indiana University, Bloomington, Indiana, USA

**ABSTRACT** Many mutualistic microbial relationships are based on nutrient cross-feeding. Traditionally, cross-feeding is viewed as being unidirectional, from the producer to the recipient. This is likely true when a producer's waste, such as a fermentation product, has value only for a recipient. However, in some cases the cross-fed nutrient holds value for both the producer and the recipient. In such cases, there is potential for nutrient re-acquisition by producer cells in a population, leading to competition against recipients. Here, we investigated the consequences of interpartner competition for cross-fed nutrients on mutualism dynamics by using an anaerobic coculture pairing fermentative *Escherichia coli* and phototrophic *Rhodospseudomonas palustris*. In this coculture, *E. coli* excretes waste organic acids that provide a carbon source for *R. palustris*. In return, *R. palustris* cross-feeds *E. coli* ammonium ( $\text{NH}_4^+$ ), a compound that both species value. To explore the potential for interpartner competition, we first used a kinetic model to simulate cocultures with varied affinities for  $\text{NH}_4^+$  in each species. The model predicted that interpartner competition for  $\text{NH}_4^+$  could profoundly impact population dynamics. We then experimentally tested the predictions by culturing mutants lacking  $\text{NH}_4^+$  transporters in both  $\text{NH}_4^+$  competition assays and mutualistic cocultures. Both theoretical and experimental results indicated that the recipient must have a competitive advantage in acquiring cross-fed  $\text{NH}_4^+$  to sustain the mutualism. This recipient-biased competitive advantage is predicted to be crucial, particularly when the communally valuable nutrient is generated intracellularly. Thus, the very metabolites that form the basis for mutualistic cross-feeding can also be subject to competition between mutualistic partners.

**IMPORTANCE** Mutualistic relationships, particularly those based on nutrient cross-feeding, promote stability of diverse ecosystems and drive global biogeochemical cycles. Cross-fed nutrients within these systems can be either waste products valued by only one partner or nutrients valued by both partners. Here, we explored how interpartner competition for a communally valuable cross-fed nutrient impacts mutualism dynamics. We discovered that mutualism stability necessitates that the recipient have a competitive advantage against the producer in obtaining the cross-fed nutrient, provided that the nutrient is generated intracellularly. We propose that the requirement for recipient-biased competition is a general rule for mutualistic coexistence based on the transfer of intracellularly generated, communally valuable resources.

**KEYWORDS** cross-feeding, coculture, fermentation, hydrogen, microbial communities, mutualism, nitrogen fixation, purple bacteria, synthetic ecology

Mutualisms, or mutually beneficial relationships between organisms, are ubiquitous and play important roles in diverse ecosystems (1). Mutualistic cross-feeding of resources between microbes can have broad impacts, ranging from influencing host health (2, 3) to driving global biogeochemical cycles (4–7). Cross-fed metabolites are

Received 4 September 2017 Accepted 25 October 2017 Published 28 November 2017

**Citation** McCully AL, LaSarre B, McKinlay JB. 2017. Recipient-biased competition for an intracellularly generated cross-fed nutrient is required for coexistence of microbial mutualists. *mBio* 8:e01620-17. <https://doi.org/10.1128/mBio.01620-17>.

**Editor** Marvin Whiteley, Georgia Institute of Technology

**Invited Editor** Matthew Mark Ramsey, University of Rhode Island

**Copyright** © 2017 McCully et al. This is an open-access article distributed under the terms of the [Creative Commons Attribution 4.0 International license](https://creativecommons.org/licenses/by/4.0/).

Address correspondence to James B. McKinlay, [jmckinla@indiana.edu](mailto:jmckinla@indiana.edu).

often regarded as nutrients due to the value they provide to a dependent partner, the recipient. However, for the partner producing the nutrient, the producer, a cross-fed nutrient's value can vary. On one extreme, the cross-fed metabolite is valued by the recipient but not the producer, as is the case for fermentative waste products (8–11). In other cases, a cross-fed metabolite holds value for both the recipient and the producer, as is the case for vitamin B<sub>12</sub> (7, 12, 13) and ammonium (NH<sub>4</sub><sup>+</sup>) (14, 15). Such communally valuable cross-fed nutrients are subject to partial privatization (16), wherein the producer has mechanisms to retain a portion of the nutrient pool for itself. While most mutualism cross-feeding studies only consider unidirectional metabolite transfer from producer to recipient, we hypothesized that partially privatized cross-fed resources could be subject to competition between partner populations. Such competition from partial privatization mechanisms seems likely, considering that competition for exogenous limiting resources is known to affect mutualism stability (9, 17–20). Similarly, others have shown that adding an exogenous source of a cross-fed nutrient can shift relationships between microbial partners from being mutualistic to competitive (21).

One example of cross-feeding that could involve competition between mutualistic partners is NH<sub>4</sub><sup>+</sup> excretion by N<sub>2</sub>-fixing bacteria (Fig. 1A), hereon called N<sub>2</sub> fixers (14, 15). During N<sub>2</sub> fixation, the enzyme nitrogenase converts N<sub>2</sub> gas into two NH<sub>3</sub> molecules (22). In an aqueous environment, NH<sub>3</sub> is in equilibrium with NH<sub>4</sub><sup>+</sup>. At neutral pH, NH<sub>4</sub><sup>+</sup> is the predominant form, but small amounts of NH<sub>3</sub> can potentially leave the cell by passive diffusion across the membrane; this passive diffusion is referred to here as NH<sub>4</sub><sup>+</sup> excretion (23) (Fig. 1B). This inherent “leakiness” for NH<sub>3</sub> likely fosters NH<sub>4</sub><sup>+</sup> cross-feeding, as extracellular NH<sub>3</sub> is available to neighboring microbes. Importantly, these neighbors can include clonal N<sub>2</sub> fixers, as NH<sub>3</sub>/NH<sub>4</sub><sup>+</sup> is a preferred nitrogen source for most microbes. At concentrations above 20 μM, extracellular NH<sub>3</sub> can be acquired by passive diffusion; below 20 μM, NH<sub>4</sub><sup>+</sup> is specifically bound and transported as NH<sub>3</sub> by AmtB transporters (Fig. 1B) (24). AmtB-like transporters are conserved throughout all domains of life (25). There is growing evidence that AmtB is used by N<sub>2</sub> fixers to recapture excreted NH<sub>3</sub> lost by passive diffusion, as ΔAmtB mutants accumulate NH<sub>4</sub><sup>+</sup> in culture supernatants, whereas wild-type strains do not (26–28). Thus, during NH<sub>4</sub><sup>+</sup> cross-feeding, AmtB likely facilitates both NH<sub>4</sub><sup>+</sup> acquisition by a recipient partner and recapture of NH<sub>4</sub><sup>+</sup> by the N<sub>2</sub> fixer.

Assessment of the effects of interpartner competition for a cross-fed nutrient would require a level of experimental control not possible in most natural settings. However, synthetic microbial communities, or cocultures, are well-suited to address such questions (29–31). We previously developed a bacterial coculture that features cross-feeding of waste products (organic acids) from *Escherichia coli* and a communally valuable nutrient (NH<sub>4</sub><sup>+</sup>) from *Rhodospseudomonas palustris* Nx (Fig. 1A) (28). We demonstrated

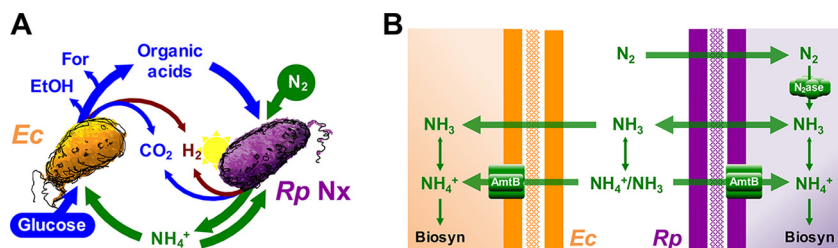


**FIG 1** An obligate bacterial mutualism based on cross-feeding of essential nutrients. (A) *Escherichia coli* (*Ec*) anaerobically ferments glucose into excreted organic acids that *Rhodospseudomonas palustris* Nx (*Rp Nx*) can consume (acetate, lactate, and succinate) and other products that *R. palustris* cannot consume (formate [For] and ethanol [EtOH]). *R. palustris* Nx grows photoheterotrophically, wherein organic compounds are used for carbon and electrons and light is used for energy. In return, *R. palustris* Nx constitutively fixes N<sub>2</sub> gas and excretes NH<sub>4</sub><sup>+</sup>, supplying *E. coli* with essential nitrogen. (B) NH<sub>4</sub><sup>+</sup> can be passively lost from cells as NH<sub>3</sub>. Both species have high-affinity NH<sub>4</sub><sup>+</sup> transporters (AmtB) that facilitate NH<sub>4</sub><sup>+</sup> uptake. NH<sub>4</sub><sup>+</sup> is the predominant form at neutral pH, as indicated by the enlarged arrowheads of the double-sided arrows.

that this coculture supports stable coexistence and reproducible growth and metabolic trends when started from a wide range of starting species ratios, including single colonies (28). Here, using both a kinetic model and genetic manipulation to alter the affinity of each species in the coculture for  $\text{NH}_4^+$ , we demonstrate that interpartner competition for excreted  $\text{NH}_4^+$  plays a direct role in maintaining coexistence. Specifically, insufficient competition by *E. coli* for  $\text{NH}_4^+$  resulted in a collapse of the mutualism. Mutualism collapse could be delayed or potentially avoided through higher  $\text{NH}_4^+$  excretion by *R. palustris* or increased *E. coli* population size. Our results suggest that for obligate mutualisms based on an intracellularly generated cross-fed nutrient, competition for that nutrient must be biased in favor of the recipient to avoid mutualism collapse and the potential extinction of both species.

## RESULTS

**Competition for cross-fed  $\text{NH}_4^+$  is predicted to shape mutualism population dynamics.** Within our coculture (Fig. 1A), *E. coli* ferments sugars into waste organic acids, providing essential carbon and electrons to *R. palustris* Nx. *R. palustris* Nx converts  $\text{N}_2$  into  $\text{NH}_4^+$  and is genetically engineered to excrete low micromolar amounts of  $\text{NH}_4^+$ , providing essential nitrogen for *E. coli* (28). The *R. palustris* parent strain does not support coculture growth with *E. coli* due to insufficient  $\text{NH}_4^+$  excretion (28).  $\text{NH}_4^+$  excretion by *R. palustris* Nx is due to a 48-nucleotide internal deletion in the gene for the master transcriptional regulator of nitrogenase, *nifA*, which results in constitutive nitrogenase activity even in the presence of normally inhibitory  $\text{NH}_4^+$  (32). In contrast to organic acids, which are only useful to *R. palustris*,  $\text{NH}_4^+$  produced by *R. palustris* Nx is essential for the growth of both species; *R. palustris* uses some  $\text{NH}_4^+$  that it converted from  $\text{N}_2$  for its own biosynthesis and excretes the rest, which serves as the nitrogen source for *E. coli*. However, *R. palustris* Nx can also take up extracellular  $\text{NH}_4^+$  (32). Thus, we hypothesized that competition for excreted  $\text{NH}_4^+$  between the *R. palustris* Nx producer population and the *E. coli* recipient population could influence mutualism dynamics.

We first explored whether competition for cross-fed  $\text{NH}_4^+$  could affect the mutualism by using SyFFoN, a mathematical model describing our coculture (28, 33). SyFFoN simulates population and metabolic dynamics in batch cocultures based on Monod equations with experimentally determined parameter values. Graphical details for individual functions and parameter value choices have been described elsewhere (33). As previous versions described  $\text{NH}_4^+$  uptake kinetics only for *E. coli* (28, 33), we amended SyFFoN to include both an *R. palustris*  $\text{NH}_4^+$  uptake affinity constant ( $K_m$ ) and a higher *R. palustris* maximum growth rate ( $\mu_{\text{MAX}}$ ) when  $\text{NH}_4^+$  is used (Fig. 2A; see also Table S1 and Text S1). Simulations from the amended model, SyFFoN v3, and the previous version, SyFFoN v2 (33), were comparable (Fig. S1). We then simulated batch cocultures, wherein the relative affinity for  $\text{NH}_4^+$  varied between the two species by increasing the  $K_m$  value for  $\text{NH}_4^+$  from the default value of 0.01 mM in either species (Fig. 2B). We did not decrease  $K_m$  values, because  $\text{NH}_4^+$  transporters are regarded as high-affinity transporters (34), and therefore we assumed that a higher affinity was less likely physiologically. The model predicted that net growth of both species is achieved only when the *R. palustris* affinity for  $\text{NH}_4^+$  is low relative to that of *E. coli* (*R. palustris*:*E. coli* affinity ratio,  $<1$ ; herein affinity values are the inverse of  $K_m$  values), as *E. coli* can acquire enough excreted  $\text{NH}_4^+$  to be able to grow. In contrast, when the *R. palustris* affinity for  $\text{NH}_4^+$  is high relative to that of *E. coli* (*R. palustris*:*E. coli* affinity ratio,  $>1$ ), *E. coli* growth is no longer supported, because *E. coli* cannot compete for excreted  $\text{NH}_4^+$ . These trends are minimally impacted by the increase in the *R. palustris* growth rate when reacquiring  $\text{NH}_4^+$  (Fig. S2). Changing the default  $K_m$  value (e.g., to 1  $\mu\text{M}$ ) affected the simulated cell density values but not the overall trends. Despite the lack of *E. coli* growth, high *R. palustris* cell densities were still predicted (Fig. 2B), due to persistent, low-level organic acid cross-feeding stemming from *E. coli* maintenance metabolism, which can support *R. palustris* growth even when *E. coli* is not growing (33). In contrast,  $\text{NH}_4^+$  cross-feeding from *R. palustris* to *E. coli* functions solely in a

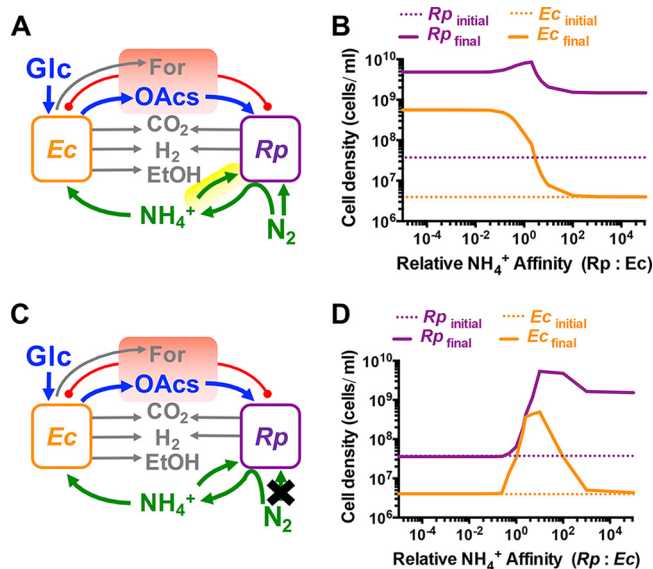


**FIG 2** Simulations suggested that *E. coli* must have a competitive advantage for  $\text{NH}_4^+$  acquisition relative to *R. palustris* to support mutualistic growth. (A) The default SyFFoN version, which enforces partial privatization of  $\text{NH}_4^+$  by allowing *R. palustris* (*Rp*) to directly use  $\text{N}_2$ . The yellow highlighted *R. palustris*  $\text{NH}_4^+$  uptake arrow is new to the default SyFFoN version used here. Red highlighting indicates that both formate (For) and consumable organic acids (OAc; succinate, lactate, and acetate) can inhibit growth and metabolism if they accumulate enough to acidify the medium. (B) Simulated population trends from the model in panel A. (C) Modified SyFFoN version where all  $\text{NH}_4^+$  made from  $\text{N}_2$  is available to both species by removing the direct utilization of  $\text{N}_2$  by *R. palustris* (black X). See Text S1 and Table S2 for more details. (D) Simulated population trends from the model in panel C. (B and D) Final cell densities (solid lines) of *R. palustris* and *E. coli* after 300 h in simulated batch cultures for a range of relative  $\text{NH}_4^+$  affinities. Starting cell densities (dashed lines) were based on a 1% dilution of cocultures containing 10% *E. coli*, as has been observed experimentally (28). Affinity is taken to be the inverse of  $K_m$ . Therefore, relative  $\text{NH}_4^+$  affinity values represent the *E. coli*  $K_m$  for  $\text{NH}_4^+$  ( $K_A$ ) divided by that of *R. palustris* ( $K_{AR}$ ). For a ratio of 1, each species had a default  $K_m$  for  $\text{NH}_4^+$  of 0.01 mM. To the left of 1, the *R. palustris*  $K_m$  value was raised. To the right of 1, the *E. coli*  $K_m$  value was raised. The peak and then decline in *R. palustris* cell density as its affinity for  $\text{NH}_4^+$  increased is an artifact of the amount of organic acids that nongrowing *E. coli* cells excreted by 300 h, as the peak was not observed when more time was simulated (Fig. S2).

growth-dependent manner, as the organic acids from *E. coli* serve both as the electron source for nitrogenase and the carbon source for *R. palustris* growth.

The SyFFoN prediction that mutualism stability requires that *E. coli* have a higher affinity for  $\text{NH}_4^+$  than does *R. palustris* might seem at odds with other models of resource competition, wherein an increased cost of cooperation and/or decreased resource capture by the cooperator (as should be the case when *E. coli* further outcompetes *R. palustris* for  $\text{NH}_4^+$ ) can result in extinction of the cooperator (35, 36). We reasoned that the population-level outcome from altering the affinity for a communally valuable nutrient depends on whether the nutrient is generated intra- or extracellularly. Intracellular generation of a communally valuable nutrient would enforce partial privatization, as the producer would have a steep advantage in retaining a sufficient portion of the nutrient pool. No matter what the recipient affinity for the nutrient, it could never overcome the advantage imparted by the physical boundary of the producer's cell envelope. Extracellular generation, on the other hand, such as the enzymatic release of sugar monomers from extracellular polysaccharides, can result in the majority of the nutrient being lost to neighboring cells, making the ability of the producer to capture the nutrient more important (35, 37). The producer advantage of intracellular nutrient generation is built into SyFFoN, as  $\text{N}_2$  and  $\text{NH}_4^+$  are treated as two separate nitrogen sources; while both species can acquire extracellular  $\text{NH}_4^+$ , there is also a direct route for  $\text{N}_2$  into an *R. palustris* biomass, bypassing  $\text{NH}_4^+$  (Fig. 2A; Text S1). To assess whether the intrinsic partial privatization provided by this direct route was responsible for the SyFFoN prediction, we modified SyFFoN so that all  $\text{N}_2$  went through  $\text{NH}_4^+$  before it could be assimilated by either species (Fig. 2C), mimicking extracellular

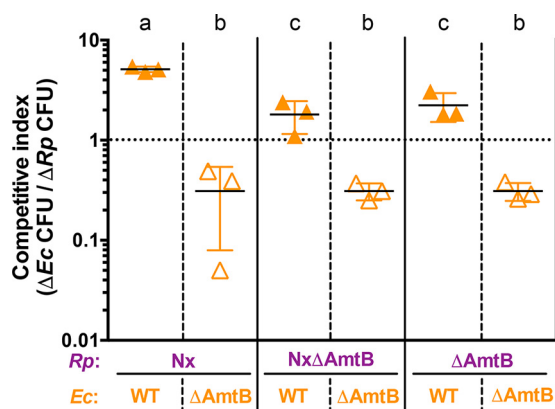


**FIG 3** AmtB is important for competitive  $\text{NH}_4^+$  acquisition. Competitive indexes for *E. coli* after 96 h in  $\text{NH}_4^+$ -limited competition assay cocultures. Cocultures were inoculated with *E. coli* and *R. palustris* at equivalent cell densities with excess carbon available for each species (25 mM glucose for *E. coli* and 20 mM sodium acetate for *R. palustris*).  $\text{NH}_4^+$  was added to cocultures to a final concentration of 5  $\mu\text{M}$  every hour for 96 h, a concentration at which AmtB is important for  $\text{NH}_4^+$  uptake (24). The dotted line indicates a competitive index value of 1, where both species are equally competitive for  $\text{NH}_4^+$ . Filled triangles, WT *E. coli*; open triangles, *E. coli*  $\Delta\text{AmtB}$ . Error bars indicate standard deviations ( $n = 3$ ). Different letters indicate statistical differences between competitive index values ( $P < 0.05$ , determined by one-way analysis of variance with Tukey's multiple-comparisons posttest).

generation of  $\text{NH}_4^+$ . In this configuration, a disproportionately high affinity for  $\text{NH}_4^+$  by either species prevented the growth of either one or both species (Fig. 2D). In the range where net growth of both species was predicted, coculture growth was dependent on preferential access by *R. palustris*, the producer rather than the recipient (Fig. 2D), similar to predictions from studies between cooperator and competitor cells (35, 37). Thus, the requirement that the *E. coli* recipient be more competitive for  $\text{NH}_4^+$  to maintain coexistence is expected to only be true for intracellularly generated  $\text{NH}_4^+$ .

**Genetic disruption of AmtB  $\text{NH}_4^+$  transporters affects relative affinities for  $\text{NH}_4^+$ .** Bacterial cells generally acquire  $\text{NH}_4^+$  through two mechanisms: passive diffusion of  $\text{NH}_3$  or uptake by AmtB transporters (Fig. 1B) (24). We hypothesized that deletion of the *amtB* gene in either species would result in a lower affinity for  $\text{NH}_4^+$  in that species and thus could be used to test how the relative  $\text{NH}_4^+$  affinity impacts coculture dynamics. We generated  $\Delta\text{AmtB}$  mutants of both *E. coli* and *R. palustris* and first characterized the effects of the mutations in monocultures. Deletion of *amtB* in *E. coli* had no effect on growth or fermentation profiles when 15 mM  $\text{NH}_4\text{Cl}$  was provided (Fig. S3), consistent with previous observations where  $\Delta\text{AmtB}$  growth defects were only apparent at  $\text{NH}_4^+$  concentrations below 20  $\mu\text{M}$  (24). In *R. palustris*  $\Delta\text{AmtB}$  monocultures with  $\text{N}_2$  as the nitrogen source, growth trends were equivalent to those of the parent strain; however, *R. palustris*  $\Delta\text{AmtB}$  excreted more  $\text{NH}_4^+$  than the parent strain and about a third of that excreted by *R. palustris* Nx (Fig. S3C and D). In line with our hypothesis,  $\text{NH}_4^+$  excretion by *R. palustris*  $\Delta\text{AmtB}$  could be due to a decreased ability to reacquire  $\text{NH}_4^+$  lost by diffusion, resulting in increased net  $\text{NH}_4^+$  excretion. Alternatively, we considered that  $\text{NH}_4^+$  excretion by *R. palustris*  $\Delta\text{AmtB}$  could be due to improper nitrogenase regulation in response to  $\text{NH}_4^+$  (27, 38). However, we found that nitrogenase activity in *R. palustris*  $\Delta\text{AmtB}$  responded similarly to  $\text{NH}_4^+$ -induced inhibition as in the parental strain (Fig. S4). These observations demonstrated that *R. palustris*  $\Delta\text{AmtB}$   $\text{NH}_4^+$  excretion is likely due to a poor ability to reacquire  $\text{NH}_4^+$  lost by diffusion.

To test our hypothesis that deletion of *amtB* would lower cellular affinity for  $\text{NH}_4^+$ , we directly tested all possible *E. coli* and *R. palustris* strain combinations in competition assays in which ample carbon was available for each species but the  $\text{NH}_4^+$  concentration was kept low. Specifically, a small amount of  $\text{NH}_4^+$  was added every hour to bring the final  $\text{NH}_4^+$  concentration to approximately 5  $\mu\text{M}$ , although it is possible that the  $\text{NH}_4^+$  concentration exceeded 5  $\mu\text{M}$  at early time points when consumption rates could have been slow due to low cell densities (Fig. 3). In this competition assay, the species



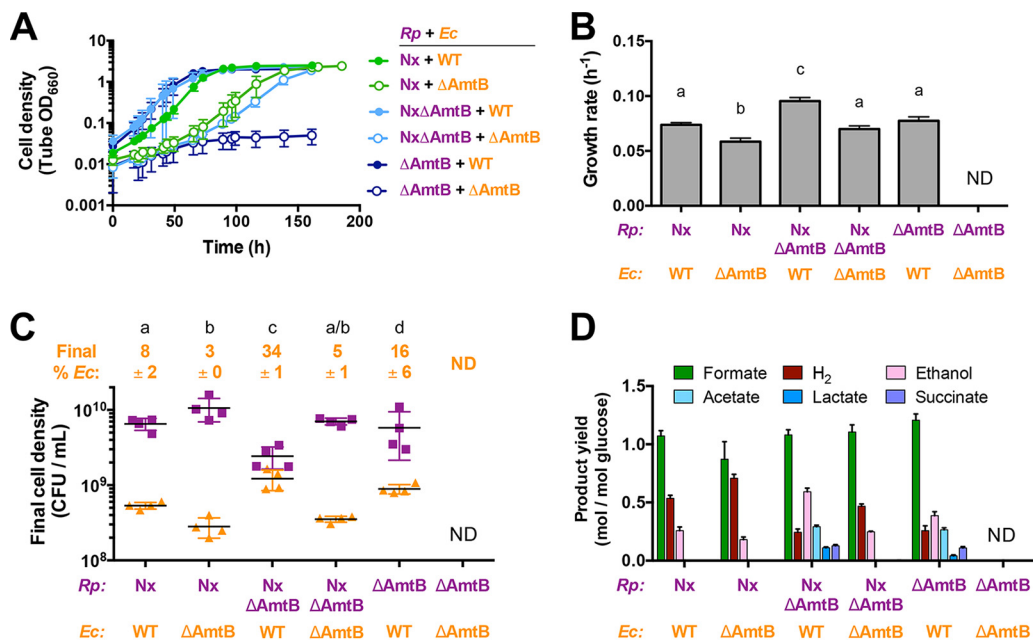


**FIG 4** AmtB influences population and metabolic trends of both partners in coculture. Growth curves (A), growth rates (B), final cell densities (C), and fermentation product yields (D) from cocultures of all combinations of mutants lacking AmtB are shown. Final cell densities and fermentation product yields were determined after 1 week, within 24 h of entering stationary phase. Cocultures were started with a 1% inoculum of stationary starter cocultures grown from single colonies that reached comparable final cell densities, as those shown in panels A and C. ND, not determined. Error bars indicate standard deviations ( $n = 4$ ). Different letters indicate statistical differences ( $P < 0.05$ , determined by a one-way analysis of variance with Tukey's multiple-comparisons posttest).

that is more competitive for  $\text{NH}_4^+$  should reach a higher cell density than the other species. In all cases, wild-type (WT) *E. coli* was more competitive for  $\text{NH}_4^+$  than any *R. palustris* strain. However, each *R. palustris* strain was able to outcompete *E. coli*  $\Delta\text{AmtB}$  (Fig. 3), even though the *E. coli* maximum growth rate is 4.6 times higher than that of *R. palustris* (Fig. S3). Even *R. palustris* strains lacking AmtB outcompeted *E. coli*  $\Delta\text{AmtB}$  (Fig. 3), indicating that *R. palustris* has a higher affinity for  $\text{NH}_4^+$  than *E. coli*, independent of AmtB. These data confirmed that deletion of *amtB* was an effective means by which to lower the relative affinity for  $\text{NH}_4^+$  in each mutualistic partner.

#### Alteration of relative $\text{NH}_4^+$ affinities affects mutualistic partner frequencies.

We then examined how relative affinities for excreted  $\text{NH}_4^+$  influenced mutualism dynamics by comparing the growth trends of cocultures containing either WT *E. coli* or *E. coli*  $\Delta\text{AmtB}$ , paired with either *R. palustris*  $\Delta\text{AmtB}$ , *R. palustris* Nx, or *R. palustris* Nx $\Delta\text{AmtB}$ , the latter of which we previously determined exhibited 3-fold-higher  $\text{NH}_4^+$  excretion levels than the Nx strain in monoculture (28). We did not use the *R. palustris* parent strain, because it was previously determined not to support coculture growth due to insufficient  $\text{NH}_4^+$  excretion (28). For each *R. palustris* partner, cocultures with *E. coli*  $\Delta\text{AmtB}$  grew slower than cocultures with WT *E. coli* (Fig. 4A and B). *E. coli*  $\Delta\text{AmtB}$  also constituted a lower percentage of the population and achieved lower cell densities than did WT *E. coli* when paired with the same *R. palustris* strain (Fig. 4C). These lower frequencies were consistent with the competitive disadvantage of *E. coli*  $\Delta\text{AmtB}$  for excreted  $\text{NH}_4^+$  (Fig. 3). AmtB is only expected to be important for  $\text{NH}_4^+$  acquisition when concentrations are below 20  $\mu\text{M}$  (24). In agreement with this expectation, supplementing cocultures with 15 mM  $\text{NH}_4\text{Cl}$  led to rapid growth and domination by *E. coli*  $\Delta\text{AmtB}$  (Fig. S5), which resembled those characteristics of previous cocultures with WT *E. coli* that were supplemented with 15 mM  $\text{NH}_4\text{Cl}$  (28). The low final cell density in cocultures with 15 mM  $\text{NH}_4\text{Cl}$  (Fig. S5) is due to rapid organic acid excretion associated with the high *E. coli* growth rate, which leads to culture acidification that prevents *R. palustris* growth (28).

For *R. palustris* strains lacking AmtB, the effects on population trends varied. Consistent with our previous work, *R. palustris* NxΔAmtB supported higher WT *E. coli* percentages and cell densities (Fig. 4C) (28). Similar to adding 15 mM NH<sub>4</sub><sup>+</sup>, the high NH<sub>4</sub><sup>+</sup> excretion level from *R. palustris* NxΔAmtB (Fig. S3D) resulted in faster *E. coli* growth and accumulation of consumable organic acids (acetate, succinate, and lactate), which acidify the medium and inhibit *R. palustris* growth (Fig. 4D) (28). Surprisingly, although *R. palustris* ΔAmtB excreted the least amount of NH<sub>4</sub><sup>+</sup> in monoculture, it supported a higher WT *E. coli* population in coculture, and consumable organic acids accumulated (Fig. 4C and D). These trends resembled those from cocultures with *R. palustris* NxΔAmtB (Fig. 4C and D). Unlike Nx strains, which have constitutive nitrogenase activity due to a mutation in the transcriptional activator *nifA* (32), *R. palustris* ΔAmtB has WT *nifA*. Thus, *R. palustris* ΔAmtB can likely still regulate nitrogenase expression, and thereby its activity, in response to nitrogen starvation. We hypothesized that in coculture with WT *E. coli*, *R. palustris* ΔAmtB might experience heightened nitrogen starvation, as NH<sub>4</sub><sup>+</sup> consumption by WT *E. coli* would limit NH<sub>4</sub><sup>+</sup> reacquisition by *R. palustris* ΔAmtB (in an *R. palustris* ΔAmtB monoculture, any lost NH<sub>4</sub><sup>+</sup> would simply benefit its clones). We therefore tested whether coculture conditions stimulated higher nitrogenase activity by using an acetylene reduction assay. In agreement with our hypothesis, *R. palustris* ΔAmtB had increased nitrogenase activity under coculture conditions compared to monocultures, whereas *R. palustris* Nx, which exhibits constitutive nitrogenase activity, showed similar levels under both conditions (Fig. S6). Thus, the relatively greater WT *E. coli* population in coculture with *R. palustris* ΔAmtB was likely due to both the competitive advantage for acquiring NH<sub>4</sub><sup>+</sup> over *R. palustris* ΔAmtB (Fig. 3) and the higher NH<sub>4</sub><sup>+</sup> cross-feeding levels associated with increased nitrogenase activity.

***E. coli* must have a competitive advantage for NH<sub>4</sub><sup>+</sup> acquisition to avoid mutualism collapse.** Unlike all other pairings, cocultures of *R. palustris* ΔAmtB paired with *E. coli* ΔAmtB showed little growth when started from a single colony of each species (Fig. 4A), a method that we routinely use to initiate cocultures (28, 33). We reasoned that the higher *R. palustris* ΔAmtB affinity for NH<sub>4</sub><sup>+</sup> relative to *E. coli* ΔAmtB (Fig. 3) likely led to community collapse, as predicted by SyFFoN (Fig. 2B). Even though SyFFoN predicted *R. palustris* growth when outcompeting *E. coli* for NH<sub>4</sub><sup>+</sup> (Fig. 2B), SyFFoN likely underestimated the time required to achieve these densities, if they would be achieved at all, as SyFFoN does not take into account cell death, which is known to occur when *E. coli* growth is prevented (33). Consistent with the hypothesis that poor coculture growth was due to a competitive disadvantage of *E. coli* ΔAmtB for NH<sub>4</sub><sup>+</sup>, SyFFoN simulations indicated that starting with a more dilute *R. palustris* inoculum would increase the probability that any given *E. coli* ΔAmtB cell would acquire NH<sub>4</sub><sup>+</sup> when in competition with *R. palustris* and thereby overcome the competitive disadvantage of *E. coli* ΔAmtB for NH<sub>4</sub><sup>+</sup> (Fig. S7). Indeed, we observed greater growth of both species when cocultures were inoculated at ratios with equal or higher relative densities of *E. coli* ΔAmtB versus *R. palustris* ΔAmtB (Fig. S7).

The explanation that mutualism collapse was due to a competitive advantage of *R. palustris* ΔAmtB over *E. coli* ΔAmtB for NH<sub>4</sub><sup>+</sup> called into question why cocultures pairing *E. coli* ΔAmtB with either *R. palustris* Nx or *R. palustris* NxΔAmtB did not collapse as well (Fig. 4), given that in all of these pairings *E. coli* ΔAmtB was at a competitive disadvantage (Fig. 3). We hypothesized that a relatively high NH<sub>4</sub><sup>+</sup> excretion level by these latter *R. palustris* strains (Fig. S3D) could compensate for a low *E. coli* NH<sub>4</sub><sup>+</sup> affinity. To explore this hypothesis, we simulated cocultures with the *R. palustris* affinity for NH<sub>4</sub><sup>+</sup> set high relative to that of *E. coli* (*R. palustris*:*E. coli* affinity ratio, 1,000) and varied the *R. palustris* NH<sub>4</sub><sup>+</sup> excretion level (Fig. 5). Indeed, increasing *R. palustris* NH<sub>4</sub><sup>+</sup> excretion was predicted to overcome a low *E. coli* affinity for NH<sub>4</sub><sup>+</sup> and support growth of both species (Fig. 5). The only exception was at the highest levels of NH<sub>4</sub><sup>+</sup> excretion, where *R. palustris* growth was predicted to be inhibited due to rapid *E. coli* growth and subsequent accumulation of organic acids that acidify the environment (Fig. 5), similar to previous observations where we experimentally increased the NH<sub>4</sub><sup>+</sup> excretion level

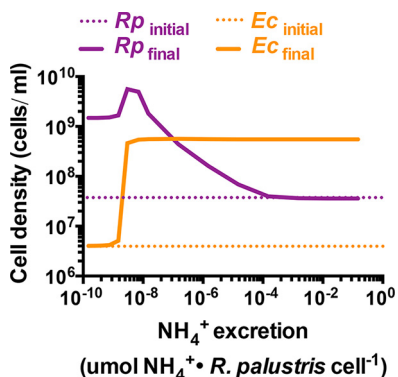


**FIG 5** Higher *R. palustris*  $\text{NH}_4^+$  excretion levels are predicted to compensate for a low *E. coli*  $\text{NH}_4^+$  affinity. Batch cultures (after 300 h) were simulated with a relative  $\text{NH}_4^+$  affinity of 1,000 (*R. palustris*:*E. coli* affinity ratio [*Rp*:*Ec*]; affinity values are the inverse of  $K_m$  values) over different *R. palustris*  $\text{NH}_4^+$  excretion levels (SyFFoN parameter  $R_A$ ). Final cell densities, solid lines; initial cell densities, dotted lines.

(28). These simulations suggested that *R. palustris* Nx and Nx $\Delta$ AmtB supported coculture growth with *E. coli*  $\Delta$ AmtB due to higher  $\text{NH}_4^+$  excretion levels (Fig. S3D), whereas a combination of low  $\text{NH}_4^+$  excretion by *R. palustris*  $\Delta$ AmtB (Fig. S3D) and a low affinity for  $\text{NH}_4^+$  by *E. coli*  $\Delta$ AmtB led to collapse of the mutualism in this pairing.

To this point, we had only considered the effect of severe discrepancies in  $\text{NH}_4^+$  affinities between the two species (e.g., a 1,000-fold difference in  $K_m$  values in our simulations) as a mechanism leading to coculture collapse within the time period of a single culturing. However, we wondered if a subtle discrepancy in  $\text{NH}_4^+$  affinities could lead to coculture collapse if given more time. We therefore simulated serial transfers of cocultures with partners having different relative  $\text{NH}_4^+$  affinities (Fig. 6A and B). At equivalent  $\text{NH}_4^+$  affinities (Fig. 6A), both species were predicted to be maintained over serial transfers. However, when the relative affinities approached a threshold (relative *R. palustris*:*E. coli* affinity ratio, 1.5), cell densities of both species were predicted to decrease over serial transfers (Fig. 6B). This decline in coculture growth is due to *E. coli* being slowly but progressively outcompeted for  $\text{NH}_4^+$  by *R. palustris*. As the difference between the *R. palustris* and *E. coli* populations expands, *R. palustris* cells have a greater chance of acquiring  $\text{NH}_4^+$  than the smaller *E. coli* population, further starving *E. coli* and simultaneously cutting off *R. palustris* from its supply of organic acids from *E. coli*.

The above prediction prompted us to investigate if cocultures pairing *R. palustris* Nx with *E. coli*  $\Delta$ AmtB were stable through serial transfers. We focused on cocultures with *R. palustris* Nx rather than *R. palustris* Nx $\Delta$ AmtB, because *R. palustris* Nx has

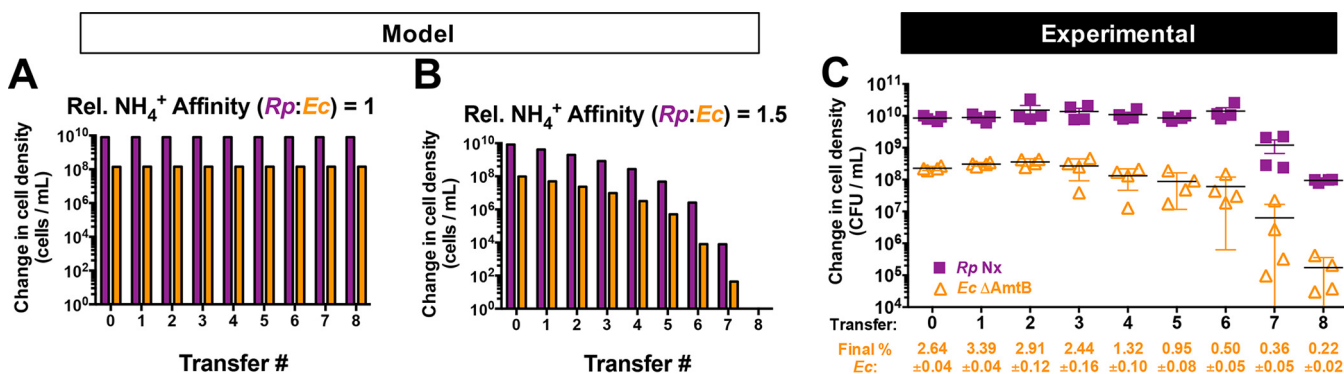


**FIG 6** A low *E. coli* affinity for  $\text{NH}_4^+$  results in coculture collapse over serial transfers when paired with *R. palustris* Nx. (A and B) Simulated batch cultures (300 h) were serially transferred using a 1% inoculum based on the cell density at 300 h for the previous culture. Relative  $\text{NH}_4^+$  affinity values represent the relative *E. coli*  $K_m$  for  $\text{NH}_4^+$  ( $K_A$ ) divided by that of *R. palustris* ( $K_{AR}$ ).  $K_A$  and  $K_{AR}$  were both 0.01 mM in panel A.  $K_A$  was 0.015 mM and  $K_{AR}$  was 0.01 mM in panel B. (C) Change in cell densities of *R. palustris* Nx and *E. coli*  $\Delta$ AmtB of cocultures grown for 1 week, less than 24 h into stationary phase. A 1% inoculum was used for each subsequent serial transfer. Error bars indicate standard deviations (SD;  $n = 4$ ). Final *E. coli* cell percentages  $\pm$  SD for each transfer are shown.



AmtB and would therefore be most likely to outcompete *E. coli*  $\Delta$ AmtB. Strikingly, over eight serial transfers of cocultures pairing *R. palustris* Nx with *E. coli*  $\Delta$ AmtB, we observed a significant decrease in cell densities of both partners (Fig. 6C). This decline in coculture growth over serial transfers was in stark contrast to results with cocultures of *R. palustris* Nx paired with WT *E. coli*, which we have serially transferred over 100 times with no extinction events (J. B. McKinlay, unpublished data). These results indicate that the recipient population must have a competitive advantage for a cross-fed nutrient relative to the producer population to avoid mutualism collapse.

## DISCUSSION

Here, we demonstrated that within a mutualistic relationship, partners can compete for a cross-fed nutrient upon which the mutualistic interaction is based, in this case  $\text{NH}_4^+$ . This competition can impact partner frequencies and mutualism stability. We demonstrated that efficient nutrient reacquisition by the producer can render nutrient excretion levels insufficient for mutualistic growth, starving the recipient and leading to tragedy of the commons (Fig. 6) (39). Conversely, recipient-biased competition for a cross-fed nutrient promotes mutualism stability. As noted above, the importance of this recipient-biased competitive advantage likely depends on whether the communally valuable resource is generated intracellularly or extracellularly (compare Fig. 2A and C). Intracellular synthesis ensures that a portion of the nutrient pool can be assimilated by the producing partner regardless of the differential affinity between the partners for that nutrient after excretion (Fig. 2A). Intracellular generation therefore helps stabilize a mutualism against an otherwise-competitive recipient by enforcing partial privatization. The competitive advantage of the recipient is in turn necessary to limit reacquisition of the excreted nutrient by the producer and thereby to drive directionality in nutrient exchange. Although partial privatization has primarily been thought to depend on mechanisms used by the producer to retain a portion of a communally valuable resource (16), our results indicate that the degree of privatization can be influenced by the partner as well; competition for the excreted nutrient pool impacts how much of a cross-fed resource will be shared versus reacquired. In effect, recipient-biased competition for an excreted communally valuable nutrient avoids tragedy of the commons by enforcing partial privatization over complete privatization.

It is expected that for mutualistic relationships based on the extracellular generation of nutrients, such as the release of sugar from a polymer, a high affinity for the nutrient by either partner can collapse the mutualism (Fig. 2D). It has been shown that microbes that excrete sugar polymer-degrading enzymes in the presence of competitors must have an advantage in obtaining the released sugars to proliferate, or even to avoid extinction (35–37). Supplementing a mutualism with an exogenous source of an otherwise-excreted communally valuable nutrient could also be viewed to mimic extracellular production. In these cases, the population outcome is also heavily influenced by the competitive affinities of each partner. For example, progressively adding exogenous nutrients to a yeast coculture stabilized by amino acid cross-feeding was shown to shift a mutualistic relationship to one of competition (21).

The importance of the recipient having the upper hand in interpartner competition likely applies to other synthetic cocultures and natural microbial mutualisms that are based on the cross-feeding of communally valuable nutrients that are generated intracellularly, including amino acids (21, 40, 41) and vitamin B<sub>12</sub> (7, 12). The same rule could also apply to interkingdom and nonmicrobial cross-feeding examples, such as those between plants and bacteria, fungi, or pollinators (1). In these cases, any decrease in resource release or emergence of traits allowing for reacquisition of a released resource would be expected to undermine the mutualism. Conversely, some nonmicrobial examples of cooperative feeding would be expected to follow the predictions for microbial mutualisms based on the extracellular generation of a communally valuable resource. For example, cooperative hunting between grouper fish and moray eels (42) or cooperative harvesting of

honey from bee hives between honeyguide birds and humans (43) would be expected to collapse if a single partner were to monopolize the resource (44). Indeed, the cooperative relationship between honeyguide birds and humans has declined in areas that have adopted bee-keeping practices, though in this case such declines are due to a technological advancement rather than evolution (43).

Our study also provided mechanistic insights into acquisition of communally valuable nutrients. AmtB transporters were shown to be crucial determinants of interpartner competition for  $\text{NH}_4^+$ . We were intrigued to find that when both species lacked AmtB, *R. palustris* outcompeted *E. coli* for  $\text{NH}_4^+$  (Fig. 5), enough to collapse the mutualism within a single culturing (Fig. 3). Whether by maximizing  $\text{NH}_4^+$  retention or reacquisition, *R. palustris*, and perhaps other  $\text{N}_2$  fixers, might have additional mechanisms aside from AmtB to minimize loss of  $\text{NH}_4^+$  as  $\text{NH}_3$ . These mechanisms could include a relatively low internal pH to favor  $\text{NH}_4^+$  over  $\text{NH}_3$ , negatively charged surface features, or relatively high affinities by  $\text{NH}_4^+$ -assimilating enzymes, such as glutamine synthetase. There are several reasons why it would be beneficial for  $\text{N}_2$  fixers to minimize  $\text{NH}_4^+$  loss. First,  $\text{N}_2$  fixation is expensive, both in terms of the enzymes involved (45) and the reaction itself, costing 16 ATP to convert 1  $\text{N}_2$  into 2  $\text{NH}_3$  (46). Passive loss of  $\text{NH}_3$  would only add to this cost, as more  $\text{N}_2$  would have to be fixed to compensate. Second, loss of  $\text{NH}_4^+$  could benefit nearby microbes competing against an  $\text{N}_2$  fixer for separate limiting nutrients (15, 47). The possibility that  $\text{N}_2$  fixers could have a superior ability to retain or acquire  $\text{NH}_4^+$ , perhaps by using mechanisms that are independent of AmtB, is not far-fetched. Bacteria are known to exhibit differential mechanisms to compete for nutrients. For example, iron acquisition commonly involves the excretion of iron-binding molecules or proteins called siderophores, which can differ in chemical structure and affinity for iron. These structural differences also influence their potential to be utilized by competitors and therefore their communal value as an extracellularly generated resource (48). Strategies to utilize siderophores as a shared resource are numerous, and they lead to different cooperative or competitive outcomes in microbial communities (48, 49). One must consider that additional mechanisms for acquiring  $\text{NH}_4^+$  beyond AmtB might likewise exist. Understanding the physiological mechanisms that confer competitive advantages for nutrient acquisition between species will undoubtedly aid in describing the interplay between competition and cooperation within mutualisms.

## MATERIALS AND METHODS

**Strains and growth conditions.** Strains, plasmids, and primers are listed in Table S2. All *R. palustris* strains contained  $\Delta uppE$  and  $\Delta hupS$  mutations to facilitate accurate CFU measurements by preventing cell aggregation (50) and to prevent  $\text{H}_2$  uptake, respectively. *E. coli* was cultivated on Luria-Bertani (LB) agar, and *R. palustris* was cultivated on defined mineral (PM) agar (51) with 10 mM succinate.  $(\text{NH}_4)_2\text{SO}_4$  was omitted from PM agar for determining *R. palustris* CFU. Monocultures and cocultures were grown in 10 ml of defined M9-derived coculture medium (MDC) (28) in 27-ml anaerobic test tubes. To make the medium anaerobic, MDC was exposed to  $\text{N}_2$  via bubbling, and then tubes were sealed with rubber stoppers and aluminum crimps and then autoclaved. After autoclaving, MDC medium was supplemented with cation solution (1% [vol/vol]; 100 mM  $\text{MgSO}_4$  and 10 mM  $\text{CaCl}_2$  stock concentration) and glucose (25 mM final concentration), unless indicated otherwise. *E. coli* monocultures were also supplemented with 15 mM  $\text{NH}_4\text{Cl}$ . All cultures were grown at 30°C laying horizontally under a 60-W incandescent bulb with shaking at 150 rpm. Starter cocultures were inoculated with 200  $\mu\text{l}$  MDC containing a suspension of a single colony of each species. Test cocultures were inoculated using a 1% inoculum from starter cocultures. Serial transfers were also inoculated with a 1% inoculum. Kanamycin and gentamicin were added to final concentrations of 100  $\mu\text{g}/\text{ml}$  for cultures of *R. palustris* and 15  $\mu\text{g}/\text{ml}$  for *E. coli* cultures when appropriate.

**Generation of *R. palustris* mutants.** *R. palustris* mutants were derived from wild-type CGA009 (52). Generation of strains CGA4004, CGA4005, and CGA4021 is described elsewhere (28). To generate strain CGA4026 (*R. palustris*  $\Delta\text{AmtB}$ ), the WT *nifA* gene was amplified using primers JBM1 and JBM2, digested with XbaI and BamHI, and ligated into plasmid pJQ200SK to make pJQnifA16. This suicide vector was then introduced into CGA4021 by conjugation, and sequential selection and screening were performed as described (53) to replace *nifA\** with WT *nifA*. Reintroduction of the WT *nifA* gene was confirmed by PCR and sequencing.

**Generation of the *E. coli*  $\Delta\text{AmtB}$  mutant.** P1 transduction (54) was used to introduce  $\Delta\text{amtB}::km$  from the Keio Collection strain JW0441-1 (55) into *E. coli* MG1655. The  $\Delta\text{amtB}::km$  genotype of kanamycin-resistant colonies was confirmed by PCR and sequencing.

**Analytic procedures.** Cell density was assayed based on the optical density at 660 nm ( $OD_{660}$ ) using a Genesys 20 visible spectrophotometer (Thermo-Fisher, Waltham, MA). Growth curve readings were obtained in culture tubes without sampling (i.e., tube  $OD_{660}$ ). Specific growth rates were determined using  $OD_{660}$  readings between 0.1 and 1.0, a range for which there is a linear correlation between cell density and  $OD_{660}$ . Final  $OD_{660}$  measurements were taken in cuvettes, and samples were diluted into the linear range as necessary.  $H_2$  was quantified using a gas chromatograph (Shimadzu, Kyoto, Japan) with a thermal conductivity detector as described (56). Glucose, organic acids, formate, and ethanol were quantified using a Shimadzu high-performance liquid chromatograph as described (57).  $NH_4^+$  was quantified using an indophenol colorimetric assay as described (28). Acetylene reduction assays (45) were performed by first harvesting cells from 10 ml of medium and resuspending in 10 ml of fresh MDC medium in 27-ml sealed tubes preflushed with argon gas. Suspensions were incubated in light for 1 h at 30°C to recover. Then, 250  $\mu$ l of 100% acetylene gas was injected into the headspace to initiate the assay, and ethylene production was measured over time by gas chromatography, as described (45). Ethylene levels were normalized to total *R. palustris* CFU in the 10-ml volume.

**$NH_4^+$  competition assay.** Fed batch cultures were prepared in custom anaerobic 75-ml serum vials with side sampling ports. Each vial contained a stir bar and 30 ml of MDC and was sealed at both ends with rubber stoppers and aluminum crimps. Each vial was supplemented with 25 mM glucose, 1% (vol/vol) cation solution, and 20 mM sodium acetate. Unlike acetic acid, which *E. coli* excretes, sodium acetate does not change the pH of the medium. Starter monocultures of each species were grown to equivalent CFU (per milliliter) in MDC containing limiting nutrients (3 mM sodium acetate for *R. palustris* and 1.5 mM  $NH_4Cl$  for *E. coli*), and 1 ml of each species culture was inoculated into the serum vials. These competition cocultures were incubated at 30°C under a 60-W incandescent bulb with stirring at 200 rpm for 96 h. Each serum vial was constantly flushed with Ar to maintain anaerobic conditions.  $NH_4Cl$  was fed from a 500  $\mu$ M  $NH_4Cl$  stock via a peristaltic pump on an automatic timer at a rate of 0.33 ml/min once an hour for a final concentration of  $\sim 5$   $\mu$ M upon each addition. The  $NH_4^+$  concentration was below the known concentration at which AmtB transporters become important for  $NH_4^+$  uptake (24). Samples were taken at 0 and 96 h for quantification of CFU.

**Mathematical modeling.** A Monod model describing bidirectional cross-feeding in batch cultures, called SyFFoN v3 (syntrophy between fermenter and fixer of nitrogen, version 3), was modified from our previous model (33) to allow for competition between *E. coli* and *R. palustris* for  $NH_4^+$  as follows: (i) an equation for the *R. palustris* growth rate on  $NH_4^+$  was added to boost the *R. palustris* growth rate when acquiring  $NH_4^+$  and (ii) the ability for *R. palustris* to consume  $NH_4^+$  was added along with an *R. palustris*  $K_m$  for  $NH_4^+$  ( $K_{AR}$ ). Default  $NH_4^+$   $K_m$  values were set to 0.01 mM for both species, to achieve a ratio of 1. To achieve higher *R. palustris* or *E. coli* relative  $NH_4^+$  affinities, the *E. coli* or *R. palustris*  $K_m$  value was raised, respectively. Simulated cultures were run for 300 h unless noted otherwise. Normally, full glucose consumption occurs by  $\sim 100$  h under typical experimental conditions and in corresponding simulations, but 300 h was allowed to capture trends that would take longer to emerge in response to parameter changes while still approximating a reasonable experimental time frame. Equations and default parameter values derived from our experimental data can be found in Text S1 and Table S1. SyFFoN v3 is run in RStudio and is available for download at <https://github.com/McKinlab/Coculture-Mutualism>.

## SUPPLEMENTAL MATERIAL

Supplemental material for this article may be found at <https://doi.org/10.1128/mBio.01620-17>.

**TEXT S1**, DOCX file, 0.1 MB.

**FIG S1**, TIF file, 0.4 MB.

**FIG S2**, TIF file, 0.2 MB.

**FIG S3**, TIF file, 0.3 MB.

**FIG S4**, TIF file, 0.3 MB.

**FIG S5**, TIF file, 0.2 MB.

**FIG S6**, TIF file, 0.1 MB.

**FIG S7**, TIF file, 0.2 MB.

**TABLE S1**, DOCX file, 0.02 MB.

**TABLE S2**, DOCX file, 0.02 MB.

## ACKNOWLEDGMENTS

We thank Richard Phillips (Indiana University) for providing equipment for the  $NH_4^+$  competition assay. We also thank Jay Lennon (Indiana University) for helpful discussions on the manuscript.

This work was supported in part by the U.S. Department of Energy, Office of Science, Office of Biological and Environmental Research, under award number DE-SC0008131, by the U.S. Army Research Office, grant W911NF-14-1-0411, and by the Indiana University College of Arts and Sciences.

The funders had no role in study design, data collection and interpretation, or the decision to submit the work for publication.

## REFERENCES

- Bronstein JL. 2001. The exploitation of mutualisms. *Ecol Lett* 4:277–287. <https://doi.org/10.1046/j.1461-0248.2001.00218.x>.
- Flint HJ, Duncan SH, Scott KP, Louis P. 2007. Interactions and competition within the microbial community of the human colon: links between diet and health. *Environ Microbiol* 9:1101–1111. <https://doi.org/10.1111/j.1462-2920.2007.01281.x>.
- Hammer ND, Cassat JE, Noto MJ, Lojek LJ, Chadha AD, Schmitz JE, Creech CB, Skaar EP. 2014. Inter- and intraspecies metabolite exchange promotes virulence of antibiotic-resistant *Staphylococcus aureus*. *Cell Host Microbe* 16:531–537. <https://doi.org/10.1016/j.chom.2014.09.002>.
- McInerney MJ, Sieber JR, Gunsalus RP. 2009. Syntrophy in anaerobic global carbon cycles. *Curr Opin Biotechnol* 20:623–632. <https://doi.org/10.1016/j.copbio.2009.10.001>.
- Durham BP, Sharma S, Luo H, Smith CB, Amin SA, Bender SJ, Dearth SP, Van Mooy BAS, Campagna SR, Kujawinski EB, Armbrust EV, Moran MA. 2015. Cryptic carbon and sulfur cycling between surface ocean plankton. *Proc Natl Acad Sci U S A* 112:453–457. <https://doi.org/10.1073/pnas.1413137112>.
- Reeburgh WS. 2007. Oceanic methane biogeochemistry. *Chem Rev* 107:486–513. <https://doi.org/10.1021/cr050362v>.
- Croft MT, Lawrence AD, Raux-Deery E, Warren MJ, Smith AG. 2005. Algae acquire vitamin B<sub>12</sub> through a symbiotic relationship with bacteria. *Nature* 438:90–93. <https://doi.org/10.1038/nature04056>.
- McInerney MJ, Struchtemeyer CG, Sieber J, Mouttaki H, Stams AJM, Schink B, Rohlin L, Gunsalus RP. 2008. Physiology, ecology, phylogeny, and genomics of microorganisms capable of syntrophic metabolism. *Ann N Y Acad Sci* 1125:58–72. <https://doi.org/10.1196/annals.1419.005>.
- Hillesland KL, Stahl DA. 2010. Rapid evolution of stability and productivity at the origin of a microbial mutualism. *Proc Natl Acad Sci U S A* 107:2124–2129. <https://doi.org/10.1073/pnas.0908456107>.
- Schink B. 1997. Energetics of syntrophic cooperation in methanogenic degradation. *Microbiol Mol Biol Rev* 61:262–280.
- Stams AJM. 1994. Metabolic interactions between anaerobic bacteria in methanogenic environments. *Antonie van Leeuwenhoek* 66:271–294. <https://doi.org/10.1007/BF00871644>.
- Grant MA, Kazamia E, Cicuta P, Smith AG. 2014. Direct exchange of vitamin B<sub>12</sub> is demonstrated by modeling the growth dynamics of algal-bacterial cocultures. *ISME J* 8:1418–1427. <https://doi.org/10.1038/ismej.2014.9>.
- Seth EC, Taga ME. 2014. Nutrient cross-feeding in the microbial world. *Front Microbiol* 5:350. <https://doi.org/10.3389/fmicb.2014.00350>.
- Behrens S, Lösekann T, Pett-Ridge J, Weber PK, Ng WO, Stevenson BS, Hutcheon ID, Relman DA, Spormann AM. 2008. Linking microbial phylogeny to metabolic activity at the single-cell level by using enhanced element labeling-catalyzed reporter deposition fluorescence in situ hybridization (EL-FISH) and NanoSIMS. *Appl Environ Microbiol* 74:3143–3150. <https://doi.org/10.1128/AEM.00191-08>.
- Adam B, Klawonn I, Svedén JB, Bergkvist J, Nahar N, Walve J, Littmann S, Whitehouse MJ, Lavik G, Kuypers MMM, Ploug H. 2016. N<sub>2</sub>-fixation, ammonium release and N-transfer to the microbial and classical food web within a plankton community. *ISME J* 10:450–459. <https://doi.org/10.1038/ismej.2015.126>.
- Estrela S, Morris JJ, Kerr B. 2016. Private benefits and metabolic conflicts shape the emergence of microbial interdependencies. *Environ Microbiol* 18:1415–1427. <https://doi.org/10.1111/1462-2920.13028>.
- Meyer JS, Tsuchiya HM, Fredrickson AG. 1975. Dynamics of mixed populations having complementary metabolism. *Biotechnol Bioeng* 17:1065–1081. <https://doi.org/10.1002/bit.260170709>.
- Kim HJ, Boedicker JQ, Choi JW, Ismagilov RF. 2008. Defined spatial structure stabilizes a synthetic multispecies bacterial community. *Proc Natl Acad Sci U S A* 105:18188–18193. <https://doi.org/10.1073/pnas.0807935105>.
- Miura Y, Tanaka H, Okazaki M. 1980. Stability analysis of commensal and mutual relations with competitive assimilation in continuous mixed culture. *Biotechnol Bioeng* 22:929–946. <https://doi.org/10.1002/bit.260220503>.
- Estrela S, Trisos CH, Brown SP. 2012. From metabolism to ecology: cross-feeding interactions shape the balance between polymicrobial conflict and mutualism. *Am Nat* 180:566–576. <https://doi.org/10.1086/667887>.
- Hoek TA, Axelrod K, Biancalani T, Yurtsev EA, Liu J, Gore J. 2016. Resource availability modulates the cooperative and competitive nature of a microbial cross-feeding mutualism. *PLoS Biol* 14:e1002540. <https://doi.org/10.1371/journal.pbio.1002540>.
- Bulen WA, LeComte JR. 1966. The nitrogenase system from *Azotobacter*: two-enzyme requirement for N<sub>2</sub> reduction, ATP-dependent H<sub>2</sub> evolution, and ATP hydrolysis. *Proc Natl Acad Sci U S A* 56:979–986. <https://doi.org/10.1073/pnas.56.3.979>.
- Walter A, Gutknecht J. 1986. Permeability of small nonelectrolytes through lipid bilayer membranes. *J Membr Biol* 90:207–217. <https://doi.org/10.1007/BF01870127>.
- Kim M, Zhang Z, Okano H, Yan D, Groisman A, Hwa T. 2012. Need-based activation of ammonium uptake in *Escherichia coli*. *Mol Syst Biol* 8:616. <https://doi.org/10.1038/msb.2012.46>.
- Peng J, Huang CH. 2006. Rh proteins vs Amt proteins: an organismal and phylogenetic perspective on CO<sub>2</sub> and NH<sub>3</sub> gas channels. *Transfus Clin Biol* 13:85–94. <https://doi.org/10.1016/j.tracli.2006.02.006>.
- Barney BM, Eberhart LJ, Ohlert JM, Knutson CM, Plunkett MH. 2015. Gene deletions resulting in increased nitrogen release by *Azotobacter vinelandii*: application of a novel nitrogen biosensor. *Appl Environ Microbiol* 81:4316–4328. <https://doi.org/10.1128/AEM.00554-15>.
- Zhang T, Yan Y, He S, Ping S, Alam KM, Han Y, Liu X, Lu W, Zhang W, Chen M, Xiang W, Wang X, Lin M. 2012. Involvement of the ammonium transporter AmtB in nitrogenase regulation and ammonium excretion in *Pseudomonas stutzeri* A1501. *Res Microbiol* 163:332–339. <https://doi.org/10.1016/j.resmic.2012.05.002>.
- LaSarre B, McCully AL, Lennon JT, McKinlay JB. 2017. Microbial mutualism dynamics governed by dose-dependent toxicity of cross-fed nutrients. *ISME J* 11:337–348. <https://doi.org/10.1038/ismej.2016.141>.
- Widder S, Allen RJ, Pfeiffer T, Curtis TP, Wiuf C, Sloan WT, Cordero OX, Brown SP, Momeni B, Shou W, Kettle H, Flint HJ, Haas AF, Laroche B, Kreft JU, Rainey PB, Freilich S, Schuster S, Milferstedt K, van der Meer JR, Grosskopf T, Huisman J, Free A, Picioreanu C, Quince C, Klapper I, Labarthe S, Smets BF, Wang H, Isaac Newton Institute Fellows, Soyer OS. 2016. Challenges in microbial ecology: building predictive understanding of community function and dynamics. *ISME J* 10:2557–2568. <https://doi.org/10.1038/ismej.2016.45>.
- Momeni B, Chen CC, Hillesland KL, Waite A, Shou W. 2011. Using artificial systems to explore the ecology and evolution of symbioses. *Cell Mol Life Sci* 68:1353–1368. <https://doi.org/10.1007/s00018-011-0649-y>.
- Lindemann SR, Bernstein HC, Song HS, Fredrickson JK, Fields MW, Shou W, Johnson DR, Beliaev AS. 2016. Engineering microbial consortia for controllable outputs. *ISME J* 10:2077–2084. <https://doi.org/10.1038/ismej.2016.26>.
- McKinlay JB, Harwood CS. 2010. Carbon dioxide fixation as a central redox cofactor recycling mechanism in bacteria. *Proc Natl Acad Sci U S A* 107:11669–11675. <https://doi.org/10.1073/pnas.1006175107>.
- McCully AL, LaSarre B, McKinlay JB. 2017. Growth-independent cross-feeding modifies boundaries for coexistence in a bacterial mutualism. *Environ Microbiol* 19:3538–3550. <https://doi.org/10.1111/1462-2920.13847>.
- Khademi S, O'Connell J III, Remis J, Robles-Colmenares Y, Miercke LJ, Stroud RM. 2004. Mechanism of ammonia transport by Amt/MEP/Rh: structure of AmtB at 1.35 Å. *Science* 305:1587–1594. <https://doi.org/10.1126/science.1101952>.
- Gore J, Youk H, van Oudenaarden A. 2009. Snowdrift game dynamics and facultative cheating in yeast. *Nature* 459:253–256. <https://doi.org/10.1038/nature07921>.
- Celiker H, Gore J. 2012. Competition between species can stabilize public-goods cooperation within a species. *Mol Syst Biol* 8:621. <https://doi.org/10.1038/msb.2012.54>.
- Drescher K, Nadell CD, Stone HA, Wingreen NS, Bassler BL. 2014. Solutions to the public goods dilemma in bacterial biofilms. *Curr Biol* 24:50–55. <https://doi.org/10.1016/j.cub.2013.10.030>.
- Yakunin AF, Hallenbeck PC. 2002. AmtB is necessary for NH<sub>4</sub><sup>+</sup>-induced nitrogenase switch-off and ADP-ribosylation in *Rhodobacter capsulatus*. *J Bacteriol* 184:4081–4088. <https://doi.org/10.1128/JB.184.15.4081-4088.2002>.
- Rankin DJ, Bargum K, Kokko H. 2007. The tragedy of the commons in evolutionary biology. *Trends Ecol Evol* 22:643–651. <https://doi.org/10.1016/j.tree.2007.07.009>.
- Pande S, Merker H, Bohl K, Reichelt M, Schuster S, de Figueiredo LF, Kaleta C, Kost C. 2014. Fitness and stability of obligate cross-feeding

- interactions that emerge upon gene loss in bacteria. *ISME J* 8:953–962. <https://doi.org/10.1038/ismej.2013.211>.
41. Harcombe W. 2010. Novel cooperation experimentally evolved between species. *Evolution* 64:2166–2172. <https://doi.org/10.1111/j.1558-5646.2010.00959.x>.
  42. Bshary R, Hohner A, Ait-el-Djoudi K, Fricke H. 2006. Interspecific communicative and coordinated hunting between groupers and giant moray eels in the red sea. *PLoS Biol* 4:e431. <https://doi.org/10.1371/journal.pbio.0040431>.
  43. Isack HA, Reyer HU. 1989. Honeyguides and honey gatherers: interspecific communication in a symbiotic relationship. *Science* 243:1343–1346. <https://doi.org/10.1126/science.243.4896.1343>.
  44. Sachs JL, Mueller UG, Wilcox TP, Bull JJ. 2004. The evolution of cooperation. *Q Rev Biol* 51:135–160. <https://doi.org/10.1086/383541>.
  45. Oda Y, Samanta SK, Rey FE, Yan T, Zhou J, Harwood CS. 2005. Functional genomic analysis of three nitrogenase isozymes in the photosynthetic bacterium *Rhodospseudomonas palustris*. *J Bacteriol* 187:7784–7794. <https://doi.org/10.1128/JB.187.22.7784-7794.2005>.
  46. Hoffman BM, Lukoyanov D, Dean DR, Seefeldt LC. 2013. Nitrogenase: a draft mechanism. *ACC Chem Res* 46:587–595. <https://doi.org/10.1021/ar300267m>.
  47. Morris JJ, Lenski RE, Zinser ER. 2012. The black queen hypothesis: evolution of dependencies through adaptive gene loss. *mBio* 3:e00036-12. <https://doi.org/10.1128/mBio.00036-12>.
  48. Joshi F, Archana G, Desai A. 2006. Siderophore cross-utilization amongst rhizospheric bacteria and the role of their differential affinities for Fe<sub>3</sub><sup>+</sup> on growth stimulation under iron-limited conditions. *Curr Microbiol* 53:141–147. <https://doi.org/10.1007/s00284-005-0400-8>.
  49. Niehus R, Picot A, Oliveira NM, Mitri S, Foster KR. 2017. The evolution of siderophore production as a competitive trait. *Evolution* 71:1443–1455. <https://doi.org/10.1111/evo.13230>.
  50. Fritts RK, LaSarre B, Stoner AM, Posto AL, McKinlay JB. 2017. A *Rhizobiales*-specific unipolar polysaccharide adhesin contributes to *Rhodospseudomonas palustris* biofilm formation across diverse photoheterotrophic conditions. *Appl Environ Microbiol* 83:e03035-16. <https://doi.org/10.1128/AEM.03035-16>.
  51. Kim M-K, Harwood CS. 1991. Regulation of benzoate-CoA ligase in *Rhodospseudomonas palustris*. *FEMS Microbiol Lett* 83:199–203. <https://doi.org/10.1111/j.1574-6968.1991.tb04440.x-1>.
  52. Larimer FW, Chain P, Hauser L, Lamerdin J, Malfatti S, Do L, Land ML, Pelletier DA, Beatty JT, Lang AS, Tabita FR, Gibson JL, Hanson TE, Bobst C, Torres JLTY, Peres C, Harrison FH, Gibson J, Harwood CS. 2004. Complete genome sequence of the metabolically versatile photosynthetic bacterium *Rhodospseudomonas palustris*. *Nat Biotechnol* 22:55–61. <https://doi.org/10.1038/nbt923>.
  53. Rey FE, Oda Y, Harwood CS. 2006. Regulation of uptake hydrogenase and effects of hydrogen utilization on gene expression in *Rhodospseudomonas palustris*. *J Bacteriol* 188:6143–6152. <https://doi.org/10.1128/JB.00381-06>.
  54. Thomason LC, Costantino N, Court DL. 2007. *E. coli* genome manipulation by P1 transduction. *Curr Protoc Mol Biol* Chapter 17:Unit 1.17. <https://doi.org/10.1002/0471142727.mb0117s79>.
  55. Baba T, Ara T, Hasegawa M, Takai Y, Okumura Y, Baba M, Datsenko KA, Tomita M, Wanner BL, Mori H. 2006. Construction of *Escherichia coli* K-12 in-frame, single-gene knockout mutants: the Keio Collection. *Mol Syst Biol* 2:2006.0008. <https://doi.org/10.1038/msb4100050>.
  56. Huang JJ, Heiniger EK, McKinlay JB, Harwood CS. 2010. Production of hydrogen gas from light and the inorganic electron donor thiosulfate by *Rhodospseudomonas palustris*. *Appl Environ Microbiol* 76:7717–7722. <https://doi.org/10.1128/AEM.01143-10>.
  57. McKinlay JB, Zeikus JG, Vieille C. 2005. Insights into *Actinobacillus succinogenes* fermentative metabolism in a chemically defined growth medium. *Appl Environ Microbiol* 71:6651–6656. <https://doi.org/10.1128/AEM.71.11.6651-6656.2005>.